PHYSICAL REVIEW A **83**, 033832 (2011)

Switching and intrinsic position bistability of soliton beams in chiral nematic liquid crystals

Jeroen Beeckman,* Abbas Madani, and Pieter J. M. Vanbrabant
Department of Electronics and Information Systems, Ghent University, Sint-Pietersnieuwstraat 41, B-9000 Ghent, Belgium

Pierre Henneaux, Simon-Pierre Gorza, and Marc Haelterman
Service OPERA-photonique, Université libre de Bruxelles, CP 194/5, 50 Avenue F.D. Roosevelt, B-1050 Brussels, Belgium

(Received 14 September 2010; published 28 March 2011)

We study theoretically and experimentally the propagation of light beams in chiral nematic liquid crystals. Despite the rather complex refractive index distribution of these crystals, their reorientational nonlinearity can compensate for diffraction, leading to robust solitonlike beams propagating along helical trajectories. We demonstrate that, due to a symmetry-breaking instability of the liquid crystal structure, these beams undergo abrupt switching and bistability, features that are of potential interest for applications to all-optical signal processing.

DOI: 10.1103/PhysRevA.83.033832 PACS number(s): 42.65.Tg, 42.70.Df, 77.84.Nh, 78.20.Jq

I. INTRODUCTION

Spatial optical solitons in nematic liquid crystals (LCs) have attracted much interest because they constitute an ideal testbed for the study of nonlinear optical phenomena and they have a strong application potential in smart optical interconnections. In most experimental studies it is the reorientational nonlinearity of LC that is exploited to obtain the self-focusing effect necessary for their generation [1]. The orientation of the average direction of the molecules (the director) is changed by the optical electric field of the light beam. A wide number of configurations have been considered in order to demonstrate spatial solitons (or nematicons [2]) in nematic LCs, initially in homeotropically aligned LC [3] and later in planar-aligned LC cells with bias voltage [4] or without bias voltage [5]. Since liquid crystal is a versatile material that can be controlled in different ways, with applied voltage, magnetic fields, or self-action of the light, different publications are devoted to the control or switching of these soliton beams [6]. Recently soliton generation was shown in chiral nematic liquid crystals [7]. These crystals exhibit a gradual twisting of the director with a pitch that can be controlled by changing the concentration of the chiral dopant. The pitch must be chosen in such a way that the twisting of the director is compatible with the direction of the alignment at the top and bottom substrates. If the alignment direction at the top and bottom is the same, the total twist angle can only be a multiple of π.

Optical bistability is an intriguing phenomenon that can appear, for example, when optical nonlinearity is present in the system. In liquid crystals, optical bistability was demonstrated in different configurations ranging from a standard LC cell [8] to a frustrated-total-reflection filter [9] to a nonlinear optical interferometer [10]. Bistable behavior of soliton generation was discussed for the first time in [11] and in liquid crystals it was reported theoretically for configurations with a bias voltage [12]. In most publications, the optical bistability lies in a distinct behavior of the nonlinear system versus input power. In this work, we observe a sharp switching in soliton propagation in the sense that the optical beam propagates completely in either the upper half or the lower half of the cell. In other words, we can define two distinct states (i.e., propagation in the upper half or lower half of the cell), and the switching between the two states occurs for very small displacements of the beam position in the cell. In addition, we demonstrate that the transition from one state to the other when the cell is displaced occurs at different positions, depending on the sense of the displacement. This means that hysteresis is occurring. In the strict sense of the word, we can consider this as bistability, because at a certain position near the middle of the cell both states can exist with exactly the same system parameters. It is important to note that bistability occurs in our system in the absence of any optical feedback, contrary to standard optical bistable devices that are based on cavities or other multiple-optical-path systems. The necessary feedback is provided by the light-induced strain of the molecular chains submitted to fixed boundary conditions. It is thus the nonlinear medium itself that provides the feedback that is necessary for the bistable behavior of the beam position. In other words, we deal here with a phenomenon of intrinsic position bistability.

We have considered the 2π-twist configuration sketched in Fig. 1. The director $\bar{n}$ is fixed at the top and bottom substrates to be along the propagation direction z and is uniformly twisted over the thickness of the cell according to the formula $\bar{n}(x,y,z) = \cos\theta\,\bar{1}_z + \sin\theta\,\bar{1}_y$, where $\theta = 2\pi x/d$ is the director angle. Note that the origin of the x axis is located at the center of the cell. A laser beam focused into this cell with polarization along the y direction experiences a refractive index profile that varies along the x direction according to $n(\theta)^2 = n_\perp^2 n_\parallel^2/[n_\perp^2\cos^2\theta + n_\parallel^2\sin^2\theta]$, where $\Delta n = n_\parallel - n_\perp$ is the birefringence of the liquid crystal, $n_\parallel$ ($n_\perp$) being the refractive index for electric field parallel (perpendicular) to the director. Accordingly, the refractive index profile exhibits two maxima located in $x = \pm d/4$, which shows that the LC cell forms two superimposed guiding layers similar to graded-index planar waveguides. However, instead of having a simple sinusoidal trajectory in either the upper or the lower guiding layer, the inhomogeneous birefringence of the chiral LC layer makes the situation a little more complex. The LC layer is indeed an anisotropic medium with a dielectric tensor $\varepsilon_{ij} = \varepsilon_\perp\delta_{ij} + \Delta\varepsilon n_i n_j$ (with $\Delta\varepsilon = n_\parallel^2 - n_\perp^2$), responsible for an x-dependent beam walkoff parallel to the yz plane. The walkoff angle α for an extraordinary polarized light beam, as considered in our experiment, is determined by $\tan\alpha = \varepsilon_{yz}/\varepsilon_{zz}$

*jeroen.beeckman@elis.ugent.be

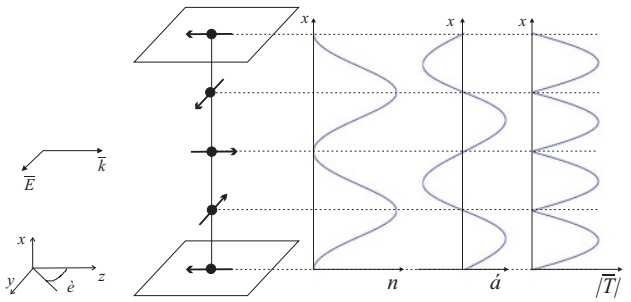

FIG. 1. (Color online) Configuration under study. The LC director is oriented along z at the top and bottom substrates and rotates over 2π over the cell thickness. In the graphs are the refractive index (n), the walkoff angle (α), and the nonlinearity of light injected along z with electric field along y.

(see Fig. 1). Due to the index gradient, a beam initially launched just above $x = 0$ propagates upward and undergoes a positive walkoff that makes it drift to the right until it reaches the position $x = d/4$, where the walkoff changes sign. The beam then continues its elevation until it starts to bend down while keeping a leftward drift. At $x = d/4$ the walkoff changes sign again and, when coming back close to $x = 0$, the beam finds its initial transverse position in both x and y. Neglecting diffraction and any imperfection, this evolution would be repeated endlessly, leading to a helical trajectory. For beams launched at a position slightly below $x = 0$, the initial walkoff is negative and the beam initially propagates to the left instead of the right. This is a simple but crucial feature which allows us to experimentally determine if the beam propagates in the upper or the lower guiding layer of the LC cell.

In addition to this inhomogeneous and anisotropic linear index distribution, the beam undergoes the reorientational nonlinearity of the LC. The strength of the nonlinearity can be measured by the torque $\bar{T}$ induced by the optical electric field $\bar{E}$ on the LC molecules. One finds $\bar{T} = \varepsilon_0 \Delta\varepsilon \langle (\bar{n} \cdot \bar{E})(\bar{n} \times \bar{E}) \rangle$, which shows that the nonlinearity is a maximum when the director angle verifies $\theta = (2k + 1)\pi/4$ and is zero when $\theta = k\pi/2$ ($k = 0, \pm 1, \ldots$) (see Fig. 1). The nonlinearity seen by a helical beam in the cell is thus strongly variable along its trajectory. However, even at the positions of maximum index $x = \pm d/4$, where the nonlinearity is zero, the effective nonlinearity averaged over the whole beam cross section is strictly positive. This makes it possible to generate nematicons near $x = \pm d/4$, as recently demonstrated by Laudyn *et al.* [7]. We can then anticipate that diffraction can be compensated by self-focusing also in the case of a helical beam launched at $x \neq \pm d/4$.

In this work, we are interested in beams that are injected close to the cell center where $\theta = 0$. Let us first consider that the beam is launched exactly at $x = 0$. In this case the upper and lower halves of the beam undergo opposite index gradient and walkoff, which tends to split the beam into two parts. The torque induced by the y-polarized electric field makes the LC molecules rotate in opposite senses on each side of the cell center. Due to molecular interaction, these opposite rotations induce a strong local strain in the LC molecular helical structure. The molecules located in the plane $x = 0$ keep their orientation $\theta = 0$ because the opposite torques due

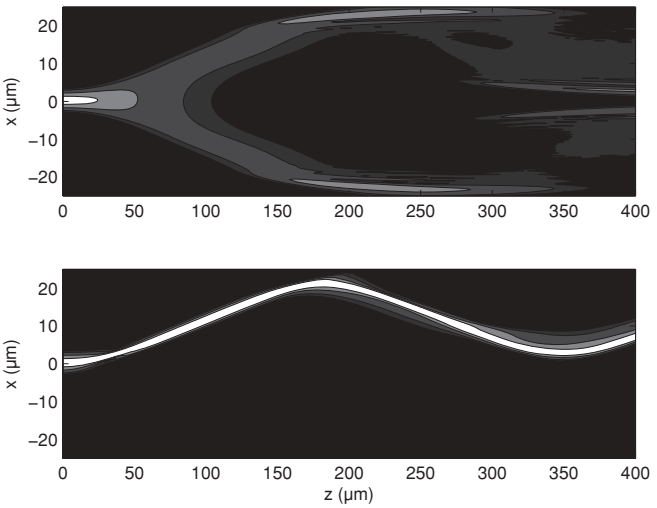

FIG. 2. Propagation of an optical beam inside the LC cell (top) without and (bottom) with nonlinearity, in the xz plane. A circular Gaussian beam with 2.5-μm waist is injected at position $x = 0.1$ μm. The beam power for the bottom graph is 45 mW.

to the interaction with the upper and lower molecules are of the same strength. However, this situation is clearly potentially unstable because the light-induced torque T is proportional to the director angle θ itself (see Fig. 1).

II. THEORETICAL ANALYSIS

A. Numerical simulations

Numerical simulations based on a realistic nonlinear beam propagation $(2 + 1)$-dimensional [$(2 + 1)$D] model similar to that of Ref. [6] are shown in Fig. 2, which displays the beam evolution in the xz plane and in Fig. 3 for the yz plane. The figures actually show an integration of the light intensity along the coordinate perpendicular to the figure. Considering the propagation in the xz plane, it can be seen that at low power the light is evenly split into the upper and lower guiding layers of

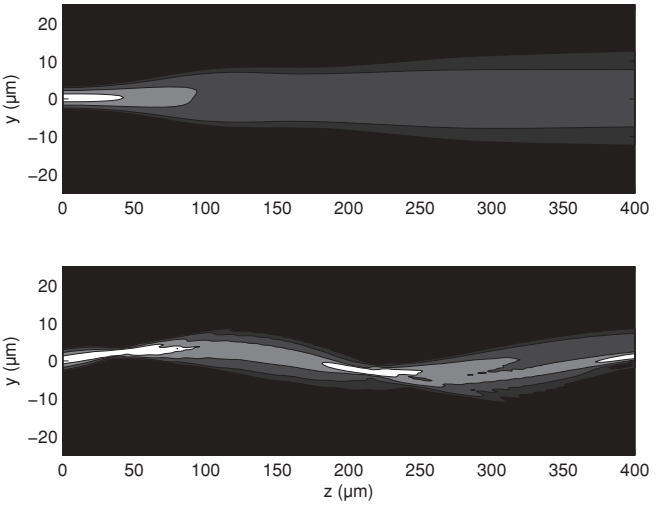

FIG. 3. Propagation of an optical beam inside the LC cell (top) without and (bottom) with nonlinearity, with the same parameters as in the previous figure, in the yz plane.

the cell. Conversely, when the optical power is large enough, the slightest asymmetric perturbation of the system results in a transfer of almost all the optical power in one of these guiding layers. The beam is undulating not only in the xz plane but also in the yz plane, as demonstrated by Fig. 3. Similar simulations for when the beam is injected at position $x = -0.1\ \mu$m confirms that the sign of the initial walkoff angle depends on the sign of the offset and hence the propagation of the soliton in either the upper or the lower guiding layer. Considering the beam propagation in all dimensions, and taking into account strong undulations in both the yz and xz planes, it is found that the solitons follow a spiraling trajectory. This is in contrast with solitons in nonchiral liquid crystals in which the soliton only undulates in one plane [13,14]. Despite the spiraling trajectory, the beam keeps its self-confinement and thus constitutes what could be called a spiraling nematicon.

B. One-dimensional model

This symmetry breaking can be captured theoretically on the basis of the one-dimensional differential equation derived from the minimization of the Oseen-Frank free energy of the LC structure [1]:

$$\frac{d^2\theta}{d\xi^2} + \alpha I(\xi)\sin 2\theta(\xi) = 0. \tag{1}$$

This equation describes the director orientation θ in the function of the light intensity distribution $I(\xi) = |\bar{E}(\xi)|^2$, where $\bar{E}$ is the electric field of light, $\alpha = \varepsilon_0\Delta\varepsilon d^2/(2K_{22})$, and K_{22} is the elastic constant for twist deformation. The transverse coordinate $\xi = 2x/d$ is scaled so that it ranges between -1 and 1. At zero light intensity the orientation of the director varies linearly as $\theta(\xi) = \pi\xi$. Hence, we can describe the director orientation as $\theta(\xi) = \pi\xi + \vartheta(\xi)$, in which ϑ expresses the deviation from the linear twisting. Equation (1) can easily be handled if the intensity can be approximated by the Dirac δ distribution, i.e., $I(\xi) = P\delta(\xi - \xi_b)$, where P is the beam power and ξ_b is the beam position. In the experiment, this means that the beamwidth has to be much smaller than the cell thickness and the LC helical pitch. In this way the angle ϑ is a piecewise linear continuous function: $\vartheta(\xi) = Q(1+\xi)/(1+\xi_b)$ for $\xi < \xi_b$ and $\vartheta(\xi) = Q(1-\xi)/(1-\xi_b)$ for $\xi > \xi_b$. The unknown coefficient Q is found by integrating the differential equation on an interval including ξ_b, which leads to the following nonlinear equation:

$$Q - \tfrac{1}{2}\left(1 - \xi_b^2\right)\alpha P \sin\left[2\left(\pi\xi_b + Q\right)\right] = 0. \tag{2}$$

We can point out that physically acceptable solutions of this equation are limited to values of light-induced angular deviation Q smaller than π. Let us first consider the symmetric configuration corresponding to a beam launched in $\xi_b = 0$. In this case, Eq. (2) reduces to $Q - \alpha P \sin(2Q)/2 = 0$. The trivial solution $Q = 0$ represents the perfectly balanced situation in which the light beam hits molecules that have a zero director angle for which the torque is zero, resulting in the absence of any deviation from the zero-intensity linear twist configuration. However, two other solutions exist provided that $\alpha P > 1$. These solutions can easily be calculated in the limit of small values of Q by using the Taylor expansion of the sine function truncated to third order. One finds $Q = \pm[3(1 - 1/\alpha P)/2]^{1/2}$. Clearly, these solutions correspond to a symmetry breaking of the helical LC structure since they lead to a reduction of either the lower or the upper guiding layer thickness. This result is illustrated in Fig. 4 through the plot of the refractive index profile. It shows that, with a symmetric illumination of sufficient power ($\alpha P > 1$), the LC structure can adopt two asymmetric configurations that are mirror images of each other. These configurations clearly result from a symmetry-breaking instability of the symmetric solution corresponding to $Q = 0$. Indeed, if the orientation of the central molecules that are hit by the laser beam is slightly perturbed from $\theta = 0$, a torque appears on these molecules that tends to increase the initial perturbation. If the power is large enough, this positive feedback induces a switching toward one of the two asymmetric solutions. If the power is too low ($\alpha P < 1$), the field is not strong enough to increase the initial perturbation and the system goes back to its initial symmetric state.

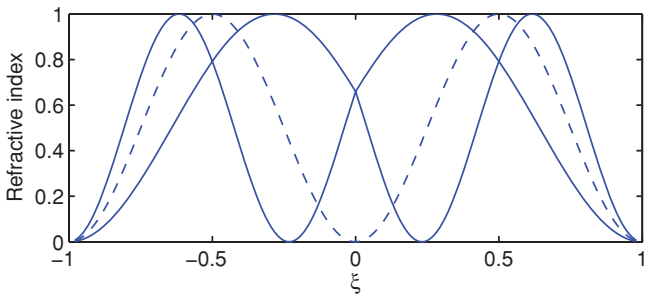

FIG. 4. (Color online) Normalized refractive index for symmetric illumination at a normalized power corresponding to $\alpha P = 2$. The dotted curve shows the symmetric solution ($Q = 0$) while the two solid curves show the mirror-image asymmetric solutions.

When the beam is launched at $\xi_b \neq 0$, a simple graphical analysis of Eq. (2) shows that the trivial solution $Q = 0$ belongs to a branch of solutions that links the two branches of asymmetric solutions on each side of the origin, resulting in a bistable cycle in terms of beam position ξ_b, as shown in Fig. 5. It is straightforward to see that bistability (i.e., the

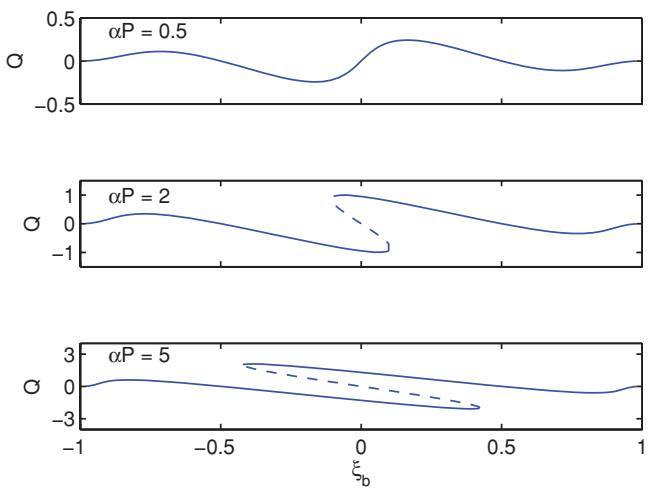

FIG. 5. (Color online) Light-induced angular deviation Q as a function of ξ_b for $\alpha P = 0.5$, 2, and 5.

coexistence of the three solutions) occurs if the slope of the curve $Q(x_b)$ at the origin is negative. Considering Eq. (2) to first order in Q and x_b shows that this slope is given by $\pi\alpha P/(1-\alpha P)$, which indicates that bistability appears as soon as the power exceeds the symmetry-breaking threshold (i.e., for $\alpha P > 1$). This symmetry-breaking behavior of the LC helix structure is represented in Fig. 5 by means of the evolution of the light-induced angular deviation Q versus ξ_b for several values of the beam power αP.

III. EXPERIMENTAL RESULTS

In order to experimentally demonstrate the symmetry breaking and the bistability, we have fabricated LC cells with 50-μm spacing between the glass plates similar to those of Ref. [4]. The glass plates are treated with a polymer alignment layer which is rubbed to ensure that the LC orientation on both glass plates is fixed along the z direction. We have used the commercial LC E7 (Merck) doped with 0.4% of chiral dopant (cholesteryl pelargonate). Tests with wedge cells (according to the technique described in Ref. [15]) have revealed that this mixture results in a helical pitch of about 50 μm, which means that the LC structure in our cell exhibits a total twist of 2π, as considered in the theory above. A glass plate is glued perpendicularly to the two confining glass plates in order to ensure a clear entrance for the laser beam [16]. The cell is fixed on a piezoelectric nanopositioning translation stage in order to control the vertical transverse beam position. Figure 6 shows the propagation of a 40-mW, 2.5-μm-wide Gaussian beam launched near the cell center (i.e., close to the point where the director lies along the z axis). The figures show the scattered light recorded by a CCD camera for four different beam positions separated by a distance of 0.5 μm. It is clearly visible that the beam is self-guided and that it follows an undulating trajectory as predicted by numerical simulations. We can also see that the resulting helical nematicon initially drifts upward Figs. 6(a) and 6(b), while it initially drifts downward Figs. 6(c) and 6(d). In order to make this clearly visible, we plotted in Fig. 6(e) the positions of the center of mass of the four beam intensity profiles as a function of the z coordinate. As explained, the sign of the initial walkoff angle determines in which of the lower or upper guiding layers the nematicon propagates. In this way we can state that the beam of Figs. 6(a) and 6(b) propagates through the upper guiding layer while the beam of Figs. 6(c) and 6(d) propagates through the lower guiding layer. Note that the only difference between Figs. 6(b) and 6(c) is an input beam displacement of 500 nm, that is, a displacement of roughly one fifth of the (half) beam width and 1% of the cell thickness. We are thus in the presence of a sharp switching effect in the sense that a minute perturbation leads to two completely distinct beam evolutions. Such a behavior may find interesting applications in the domain of all-optical signal processing.

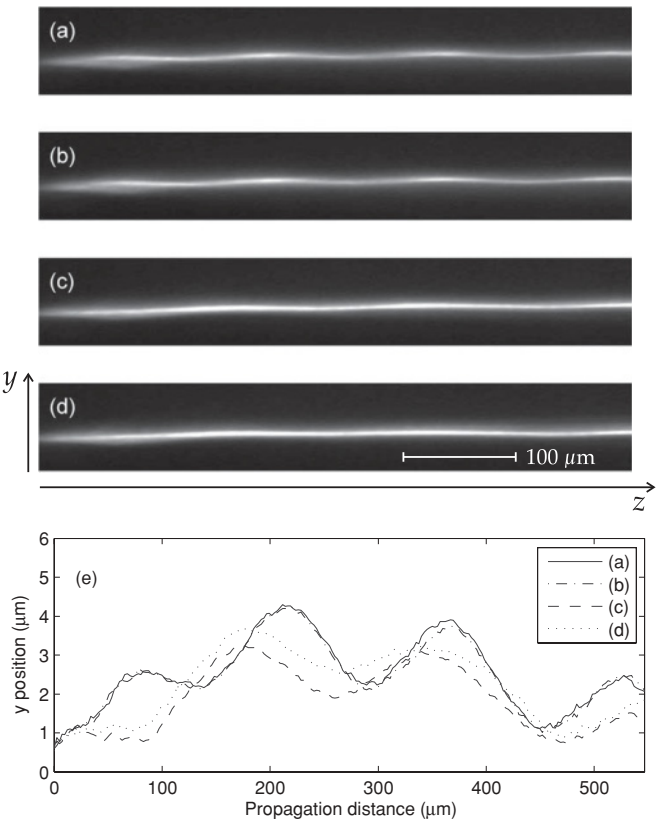

FIG. 6. Experimental observation of the propagation of an optical soliton (40 mW optical power). The beam is launched near the middle of the cell. (a)–(d) Density plot of the nematicon intensity for four beam positions separated by 0.5 μm. (e) Evolution of the beam center position as a function of the propagation coordinate z.

In order to demonstrate that this peculiar switching behavior is due to the symmetry-breaking instability of the LC helical structure, we investigated the bistable cycle associated with this instability. The bistability has been experimentally investigated by observing the initial beam walkoff angle for different input beam positions separated by 500 nm and at a fixed power of 40 mW. The initial walkoff angles were calculated from the z evolution of the center of mass of the

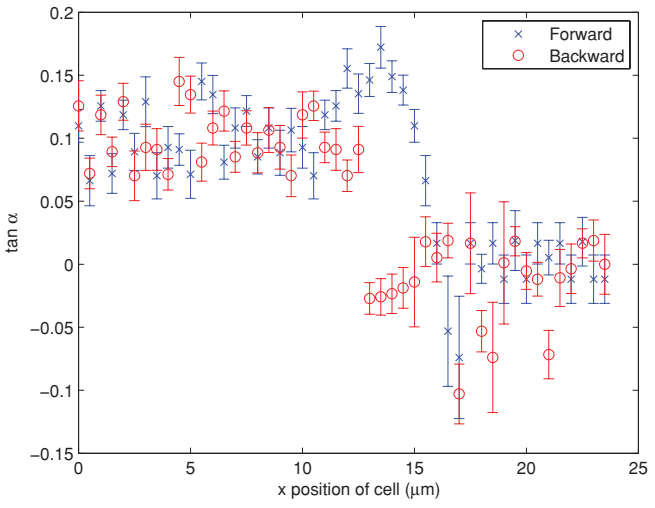

FIG. 7. (Color online) Angle of the beam entering the cell in the function of the displacement of the cell along the z axis. The angle exhibits a discontinuity for which the optical beam propagates either in the upper or the lower half of the cell. The discontinuity appears at different z position depending on the direction in which the cell is displaced.

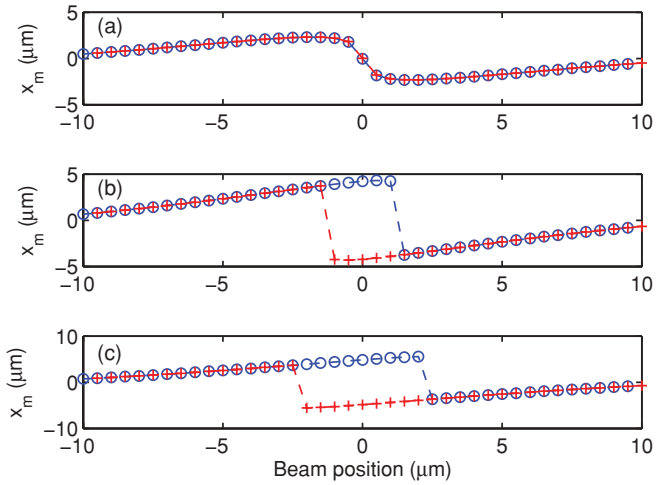

FIG. 8. (Color online) Numerical simulation of the midpoint x_m of the helical structure for different optical power: (a) 20, (b) 36, and (c) 45 mW. The data points marked with circles (crosses) are for a beam which is displaced upward (downward).

beam intensity profile see Fig. 6(e). As can be seen in Fig. 7, a clear down-switching from positive to negative walkoff angle was observed when the beam position was displaced upward, starting well beneath the cell center. At a distance of 10 μm after the down-switching point, the beam displacement direction was inverted. An up-switching can be seen at a beam position significantly smaller than that of the down-switching, resulting in a well open bistable cycle. The typical distance between up- and down-switching is 2.5 μm at a beam power of 40 mW.

The full $(2+1)$D numerical simulation model used in Figs. 2 and 3 allows us to validate our interpretation of the experimental results as well as our 1D analytical approach to the problem. The twist angle θ is calculated with the two-dimensional model for a Gaussian beam of 2.5 μm waist launched at an offset of ± 10 μm with respect to the middle of the LC layer. This twist angle distribution is calculated, after which the beam is shifted over a distance of 0.5 μm and the twist angle is relaxed from the previous solution. This procedure is repeated until the beam reaches the ∓ 10 μm position. The calculation is performed for both increasing and decreasing positions along x. The position x_m along the x axis for which the twist angle is equal to zero is the parameter used to quantify the behavior of the LC. At this position the refractive index of the LC is a minimum. Figure 8 shows the evolution of x_m in the function of the beam position for different optical power. Similar to the results in Fig. 5, no bistable cycle can be observed for low optical power, whereas high optical power results in the bistability of x_m. The bistability window is equal to a few micrometers for optical powers that are comparable to the power used in the experiment, which confirms our interpretation of the experimental findings.

IV. CONCLUSIONS

In conclusion, due to their reorientational nonlinearity and their complex refractive index distribution, chiral nematic LC cells support the propagation of undulating solitonlike beams, or nematicons. We have demonstrated that, above a power threshold, these nematicons undergo a symmetry-breaking instability associated with the appearance of bistability as experimentally demonstrated and theoretically shown from a model derived from the minimization of the Oseen-Frank free energy of the helical LC structure. Symmetry breaking, bistability, and switching are features of great potential interest for applications to all-optical signal processing and reconfigurable optical interconnects.

ACKNOWLEDGMENTS

J. Beeckman and P. J. M. Vanbrabant thank the Research Foundation Flanders for financial support. The work has been carried out in the framework of the IAP6-10 project Photonics@be of the Belgian Science Policy.

[1] I. Khoo, *Liquid Crystals*, 2nd ed., Wiley Series in Pure and Applied Optics (Wiley, New York, 2007).
[2] G. Assanto, M. Peccianti, and C. Conti, Opt. Photonics News **14**, 44 (2003).
[3] M. Karpierz, M. Sierakowski, M. Swillo, and T. Wolinsky, Mol. Cryst. Liq. Cryst. **320**, 157 (1998).
[4] M. Peccianti, A. De Rossi, G. Assanto, A. De Luca, C. Umeton, and I. Khoo, Appl. Phys. Lett. **77**, 7 (2000); J. Beeckman, K. Neyts, X. Hutsebaut, C. Cambournac, and M. Haelterman, Opt. Express **12**, 1011 (2004).
[5] M. Peccianti, C. Conti, G. Assanto, A. De Luca, and C. Umeton, Nature **432**, 733 (2004); M. A. Karpierz, M. Sierakowski, and T. R. Wolinski, Mol. Cryst. Liq. Cryst. **375**, 313 (2002).
[6] A. Piccardi, A. Alberucci, U. Bortolozzo, S. Residori, and G. Assanto, Appl. Phys. Lett. **96**, 071104 (2010); J. Beeckman, K. Neyts, and M. Haelterman, J. Opt. A: Pure Appl. Opt. **8**, 214 (2006); A. Alberucci, A. Piccardi, U. Bortolozzo, S. Residori, and G. Assanto, Opt. Lett. **35**, 390 (2010); A. Alberucci, M. Peccianti, and G. Assanto, *ibid.* **32**, 2795 (2007); Y. V. Izdebskaya, V. G. Shvedov, A. S. Desyatnikov, W. Krolikowski, and Y. S. Kivshar, *ibid.* **35**, 1692 (2010); J. Henninot, J. Blach, and M. Warenghem, J. Opt. A: Pure Appl. Opt. **9**, 20 (2007).
[7] U. Laudyn, M. Kwasny, and M. Karpierz, Appl. Phys. Lett. **94**, 091110 (2009); K. Jaworowicz, K. A. Brzdakiewicz, M. A. Karpierz, and M. Sierakowski, Mol. Cryst. Liq. Cryst. **453**, 301 (2006); M. Laudyn, U. A. Kwasny, K. Jaworowicz, K. Rutkowska, M. Karpierz, and G. Assanto, Photon. Lett. Poland **1**, 7 (2009).
[8] I. C. Khoo, Appl. Phys. Lett. **41**, 909 (1982).
[9] M. Haelterman and C. Waelbroeck, Appl. Phys. Lett. **56**, 512 (1990).
[10] U. Bortolozzo, L. Pastur, P. L. Ramazza, M. Tlidi, and G. Kozyreff, Phys. Rev. Lett. **93**, 253901 (2004).

[11] A. E. Kaplan, Phys. Rev. Lett. **55**, 1291 (1985).
[12] M. A. Karpierz, Phys. Rev. E **66**, 036603 (2002).
[13] J. Beeckman, K. Neyts, X. Hutsebaut, C. Cambournac, and M. Haelterman, Opt. Quantum Electron. **37**, 95 (2005).
[14] M. Peccianti, A. Fratalocchi, and G. Assanto, Opt. Express **12**, 6524 (2004).
[15] I. Dierking, *Textures of Liquid Crystals* (Wiley-VCH, Weinheim, 2003).
[16] A. De Luca, G. Coschignano, C. Umeton, and M. Morabito, Opt. Express **14**, 5548 (2006).